HARD KNOCK FOR DEVELOPING HIGH-ENERGY-DENSITY FERROMAGNETIC BULK AMORPHOUS ALLOYS

S. Ram

Materials Science Centre, Indian institute of Technology, Kharagpur-721302

ABSTRACT

Development in bulk amorphous alloys is reviewed. R-Fe-Al and R-Fe-Ga series and derivatives, of the ferrous system showing $(JH)_{max}$ of 10 to 20 kJ/m^3 at room temperature comparable to those of the well known rare-earth (R) magnets of $R_2Fe_{14}B$ and similar intermetallics have been dealt with along with suitable formalism for the high values. Methods of synthesis of bulk amorphous structure like rapid quenching, mechanical milling, arc melting, copper mould casting and water quenching have also been discussed.

INTRODUCTION

Till recently a reasonably high value of energy-product of the order of a few kJ/m^3 to a few hundreds kJ/m^3, was attributed to high value of magnetocrystalline anisotropy H_a in certain crystalline solids of hexagonal ferrites and $R_2Fe_{14}B$, RM_5, or R_2M_{17} intermetallics (with R as a rare-earth element and M a transition metal)[1-12]. In principle, an assembly of ideal single domain particles of size Dc has an optimal $(JH)_{max}$ value[13,14]. In conventional hard magnets of intermetallics, the value of Dc lies between 20 to 100 nm. Soft magnets of pure Fe, Co, or Ni metal (crystalline) have a similar Dc ~ 20 nm[13]. Irrespective of H_a value, both the soft and hard magnets develop a superparamagnetic character at D below Dc while a multidomain character at D above Dc. In principle, coercivity H_c, which determines the $(JH)_{max}$, has a zero value in superparamagnetic as well as multidomain particles. Shape anisotropy H_b is another important parameter which controls H_c or $(JH)_{max}$ in Dc particles[4,13]. A value of H_c as large as 50 kA/cm has been observed easily in high-energy-density (HED) rare-earth magnets with the help of Ha of 100 to 500 kA/m[13].

Values of $(JH)_{max}$ 10 to 20 kJ/m^3 at room temperature, has been observed in a new series of bulk amorphous R-Fe-Al and R-Fe-Ga alloys[15-18] opening out scope for (i) newer ferrous bulk amorphous magnetic materials (ii) understanding the basic mechanism and (iii) formalism of magnetism in disordered and ordered crystalline solids . Being characteristically isotropic in nature, the amorphous magnets find new applications in electronic and optical devices[12,18]. Methods to synthesize amorphous structure like the rapid quenching, elemental milling, arc melting, copper mould casting and water quenching are discussed.

X-ray diffraction , thermal analysis and metallographic techniques have been employed to study the amorphous phase in representative samples prepared by different methods to understand and model a formalism for the unusual magnetic properties in a bulk amorphous structure. Hard ferromagnetic properties did not persist in thin ribbons , powdering or recrystallized alloys.

EXPERIMENTAL DETAILS

The amorphous bulk alloys were prepared by (i) rapid quenching, (ii) mechanical milling from the elemental powders, (iii) arc melting, (iv) copper mould casting, and (v) water quenching. In method (i), alloy ingots prepared from pure R, Fe and Al by arc melting in argon atmosphere . Remelting of the ingots was done by cutting to 1 to 3 mm size to ensure chemical homogeneity. Milling of mixture of metal powders and the other methods of synthesis mentioned also gave bulk amorphous sturcuture[15-20].

The chemistry of bulk amorphous R-Fe-Al and R-Fe-Ga alloy phase in all cases was analyzed employing X-ray, SEM, TEM (with electron microprobe). The thermal stability of the amorphous structure was determined by the analysis of the structural parameters ,$DT = T_m - T_x$, (which was 90 K), and T_m/T_x ratio (which was as high as 0.9). T_m and T_x are respectively the onset of melting and recrystallization temperatures. Magnetic properties like saturation magnetization J_s, H_c, J_r, and Curie temperature T_C were studied with the help of a vibrating sample magnetometer. Other experimental details were the same as reported earlier[6-12].

RESULTS AND DISCUSSION

Developments in bulk amorphous alloys

The new development of bulk glass forming metallic alloys (Table 1) within the last few years has led to interesting advances in the science and technology of liquid metals. The first liquid metal alloy, as vitrified by rapidly cooling (10^5-10^6 K/s) from molten state to the glass transition, was reported in the Au-Si system by Klement et al in 1960[21]. The work of Turnbull and his group in the early 1960s was another critical contribution in this series. They developed rapidly quenched Au-Si glasses as well as other Pd-Si and Pd-Cu-Si alloys[22,23]. The field of metallic glasses gained momentum in the early 1970s when researchers at Allied chemicals developed continuous casting processes for commercial manufacture of metallic glass ribbons and sheets[24]. In this period, Chen and group explored simple suction casting methods to form bulk amorphous Pd-Cu-Si rods in millimeter diameter at 10^3 K/s moderate cooling rate[25]. This is the first example of the bulk glasses. Beginning in 1982, Turnbull, Drehman, Kui, Greer and others[26,27] developed Pd –Ni-P bulk glasses with fluxing methods. Ingots of size up to 1 cm formed in a borosilicate glass flux at10 K/s cooling rate. Lee and Johnson fabricated spherical Au-Pb-Sb droplets (amorphous) of millimeter diameter by drop tube experiments[28].

During the late 1980s, Inoue and colleagues investigated fabrication of multicomponent La-Al-Cu, Mg-Y-Cu, La-Al-Ni-Cu, Zr-Al-Cu-Ni and other similar bulk amorphous alloys using metal mould casting [29-31]. These are available in form of rods, bars and strips with dimension in the 1 to 10 mm range. Later, Peker and Johnson developed a number of Zr-Ti base alloys in a deliberate search for bulk glass forming materials. This led to the discovery of bulk glasses in the Zr-Ti-Ni-Cu-Be, Zr-Ti-Ni-Cu and related systems[32,33]. A cooling rate of 1 K/s has been found sufficient to produce fully amorphous alloys in rods of 50 mm diameter by pouring the melt into copper moulds.

Table 1 : Development in bulk amorphous alloys

A. Nonferrous alloys (weak or nonmagnetic) :	*Years*
Pd-Cu-Si	1974
Pd-Ni-P	1982
Au-Pb-Sb	1982
Mg-R-M (M : Ni, Cu or Zn)	1988
R-A1-TM (TM: VI-VIII group metal)	1989
R-Ga-TM	1989
Zr-Al-TM	1990
Zr-Ti-Al-TM	1990
Ti-Zr-TM	1993
Zr-Ti-TM-Be	1993
Zr-(Nb, Pd)-Al-TM	1995
Pd-Cu-Ni-P	1996
Pd-Ni-Fe-P	1996
Pd-Cu-B-Si	1997
Ti-Ni-Cu-Sn	1998
B. Ferrous alloys (ferromagnetic) :	
Fe-(Cu, Mn, Si etc.)-B	1985
Fe-Nd	1989
Fe-(Al, Ga)- (P, C, B, Si, Ge)	1995
Fe-(Nb, Mo)-(Al, Ga)-(P, B, Si)	1995
R-Fe-Al and or R-Fe-Ga	1995*
Co-(Al, Ga)-(P, B, Si)	1996
Fe-(Zr, Hf, Nb)-B	1996
Co-Fe-(Zr, Hf, Nb)-B	1996
Ni-(Zr, Hf, Nb)-(Cr, Mo)-B	1996
Fe-Co-R-B	1998*
Fe-(Nb, Cr, Mo)-(P,C,B)	1999
Ni-(Nb, Cr, Mo)-(P, B, Si)-B	1999

**Hard ferromagnets depending on the composition and microstructure.*

Several ferrous alloys have been developed in early 1980s in the Fe-B, Fe-B-Si and related systems but those are limited to thin ribbons only[18,34]. As mentioned above, hard ferromagnetic bulk amorphous alloys of R-Fe-Al and R-Fe-Ga systems[15-18] were introduced only in 1995. According to the pioneer work of Inoue and co-workers, this series has an exceptionally large glass forming ability (GFA). Fully X-ray amorphous and hard ferromagnetic rods of R-Fe-Al and R-Fe-Ga alloys were produced in as large diameter as 12 mm by suction casting at moderate 10 to 0.1 K/s cooling rate.

X-ray diffractogram and microstructure

The hard ferromagnetic bulk alloys of R-Fe-Al or R-Fe-Ga easily form in an amorphous structure over a large range of compositions if cooling is done from the melt in an inert atmosphere even at a slow 10 to 0.1 K/s rate. No significant devitrification appears during cooling the specimen in a dimension of 3 to 5 mm. X-ray amorphous structure is, therefore, easily achieved in alloys produced by various kinds of solidification techniques mentioned[15-23]. The mechanical attrition of an elemental mixture in a controlled atmosphere, used in the present study, gave an altogether different away of vitrifying without involving melting. Addition of volatile hydrocarbon liquid during attrition significantly helped vitrification to refined amorphous structure facilitating the reaction between the refined metal particles with nascent surfaces. Finely divided loose powder of vitrified alloy resulted.

Fig. 1 compares X-ray diffractograms in $Nd_{57}Fe_{20}Co_5Al_{10}B_8$ alloys prepared by (a) milling of mixture of pure elements (b) milling of the prealloyed ingot (c) arc melting (d) melt spinning to thin ribbon and (e) copper mould casting in the form of thin rods or cylinders. As summarized in Table 2, three broad diffraction halos q_1, q_2 and q_3, characteristic of amorphous struture[35,36], appear in the samples in (a) to (d). Only one halo at $q_1 = 14.9\ nm^{-1}$ remains in (e) the cast rod or cylinder (3 mm diameter) in part of surface devitrification into nanocrystallites due to a-Nd and $NdFe_2$. A minor variation in the positions in the three halos indicates minor changes in the local amorphous structures in the alloys due to the difference in methods of preparation. This accounts for the variations in the magnetic and other properties that depend on the local structure.

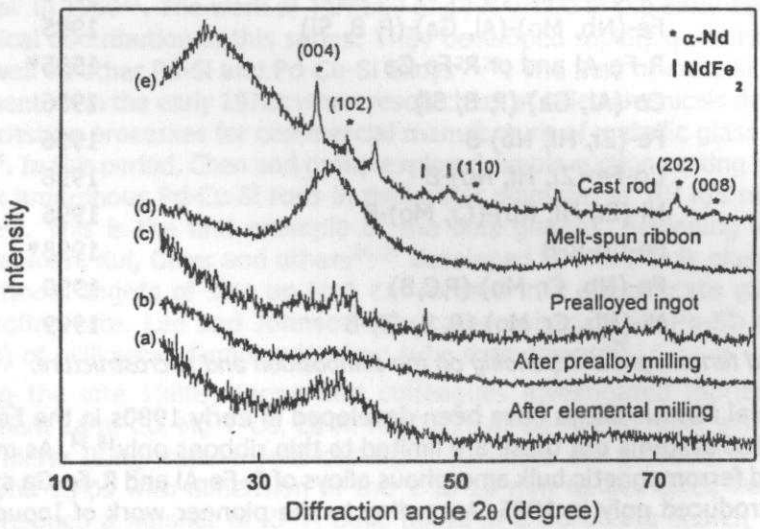

Fig. 1: X-ray diffraction in $Nd_{57}Fe_{20}Co_5Al_{10}B_8$ alloys prepared by (a) elemental milling, (b) prealloy milling, (c) arc melting, (d) melt spinning, and (e) copper mould casting.

Table 2 : The diffraction halos in $Nd_{57}Fe_{20}Co_5Al_{10}B_8$ alloys prepared by different methods

Sample	Wavevectors (nm^{-1})		
	q1	q2	q3
1. Milled elemental powder	12.8	22.9	38.2
2. Milled prealloy	13.4	23.2	38.9
3. As-prepared ingot*	12.8	22.2	39.3
4. Malt-spun ribbon	12.8	22.2	37.7
5. Copper mould cast rods**	12.9	-	-

** As prepared ingots by arc meting have a significant volume fraction of devitrified surfaces.*

** The cast rods have some a-Nd and NdFe2 nanocrystallites co-precipitated during the casting.*

In general, the samples obtained through mechanical attrition or melt spinning have smaller q_i values (larger interatomic distance $d = \lambda/2\sin\theta$ @ $2\pi q^{-1}$ as per the Bragg's law $2d\sin\theta = \lambda$) compared with others. This implies a relatively large amount of excess energy $\Delta\varepsilon$ (or enthalpy ΔH) being stored over the equilibrium value e0 in structural imperfections and defects. The excess $\Delta\varepsilon$ or ΔH results in an excess volume ΔV of the sample as per the first law of thermodynamics. This excess ΔV releases in a broad exothermic structural relaxation signal during heating of the sample in a thermal analyzer.

In the attrition process of a mixture of R, Fe and Al metal powders of predetermined composition, ball-powder-ball and ball-powder-container collisions repeatedly occur and plastically deform, cold-weld, and fracture the powder particles. Strain hardening and fracture of particles during collisions create new surfaces by a decrease of one or more dimensions depending upon the experimental conditions. When two or more refined surfaces come in contact react they react instantly by dissolution of one component into other(s), and result in a vitrified alloy. The process is called mechanical alloying. The SEM micrograph indicates a layered structure of alloy formed by a peculiar reaction within the components and cold welding of latter layer by layer as reported earlier in milling of a pure iron powder[19].

Monolayers of the alloy get as thinned as possible in the continuous collisions during the attrition process. Usually the microstructure on attrition of pure metals[19] shows a definite thickness (t), which appears to be smaller than the critical diameter (D) in a stable crystallite of it, i.e., $t<D$. Instantaneous cold-welding of a freshly created nascent layer structure over a stable layer supports its originally thin-layered structure. As a result, the material in the thin layer does not recrystallize easily in course of extended milling and the final sample ultimately attains an amorphous structure in individual layers, which arrange one over the other. TEM micrographs and electron diffraction pictures of selected samples were analyzed along with their compositional maps. It was found that a single amorphous structure, in the average alloy composition, appears throughout the specimen with a characteristic broad diffraction ring at $q_2 = 22.7\ nm^{-1}$, as observed in the X-ray diffractogram.

A peculiar microstructure of separated domains or clusters appeared in acicular or spherical shapes of the alloys obtained by the arc melting or the copper mould casting. They have distinct structures with defined boundaries in phase-separated regions. Some small crystallites were visible in the liquid-liquid phase separated regions. It appears that the alloy components are peculiarly highly soluble into one another and thus easily form a single stable homogeneous melt. The melt, therefore, easily retains its liquid structure even if cooling is slowly (~1 K/s) as in thin ingot casting.

Phase diagram and strong glass formability

As mentioned above, the $Nd_{90-x}Fe_xAl_{10}$ easily forms amorphous phase (over wide range of x) in mechanical attrition, copper mould casting or arc melting process. For example, DSC thermogram for a typical x = 30 alloy, obtained in small ingots of 3 to 5 mm diameter by the arc melting, has a broad exothermic peak over 500 t0 750 K (with a change of enthalpy DH1 =12 J/g) followed by a strong exothermic peak at Tp =795 K (with enthalpy DH2 =35 J/g) with T_x = 763 K and T_m= 910 K. The present T_x and T_m values are in a fairly good agreement with the values reported by other methods. The first signal is a characteristic structural relaxation signal with a large ΔH_1 =12 J/g excess energy retained in the alloy above the equilibrium state e0. The mechanical attrition process results in a presumably further larger value of ΔH_1 =15 J/g (with T_p = 800 K, T_x = 760 K and T_m= 915 K) stored in the alloy in form of an excess energy in structural imperfection and defects with an enhanced volume in the deformed structure in thin layers.

The values for T_x and T_m for the selected R-Fe-Al alloys are given in Table 3. The temperature interval, $\Delta T_m = T_m - T_x$, of the supercooled liquid defined by the difference between T_m and T_x is as small as 90 K and the reduced crystallization temperature $F = T_x/T_m$ is as high as 0.9. The small ΔT_m and large F values seem to be responsible for the large GFA in these alloys.

Table 3 : Thermal stability data in hard ferromagnetic bulk amorphous R-Fe-Al alloys

Composition	Thermal stability*			
	T_x(K)	T_m(K)	$\Delta T_m = T_m - T_x$	$\Phi = T_x/T_m$
$Nd_{70}Fe_{20}Al_{10}$	750	866	116	0.87
$Nd_{60}Fe_{30}Al_{10}$	763	910	147	0.84
$Pr_{60}Fe_{30}Al_{10}$	765	855	90	0.90
$Er_{60}Fe_{30}Al_{10}$	820	950	130	0.86

** The data are deduced from DSC thermograms measured at 0.33 K/s heating.*

A large GFA in this system, leading to the formation of bulk amorphous alloy, originates from the high thermal stability of the liquid (or solid solution) against crystallization at T_x or above. It can be described by the temperature interval, $\Delta T_x = T_x - T_g$, of the supercooled liquid region before crystallization, where T_g is its glass

transition temperature. Inoue et al[17,18] studied the compositional dependence of ΔT_x for a series of R-Fe-Al amorphous alloys. As can be derived from the Hume-Rothery's rules of alloying[37], the large GFA in this series satisfies four empirical rules, (i) alloy systems consisting of multicomponents, (ii) significantly different atomic size ratios above 12% among the main constituent elements, (iii) a large negative heat of mixing among the constituent elements, and (iv) a large macroscopic interaction among the components to arrange in a polymeric structure. The fourth rule proposed in this investigation governs with the existence of a relatively large value of viscosity in this series. The instantaneous value of the viscosity plays a crucial role in undercooling the liquid through a continuous growth of it at moderate rate as a function of cooling so that it slowly reaches to an immobile glassy state at Tg.

The factor (iv) explains the existence of a large GFA in a multicomponent system in combination with the other (ii) and (iii) parameters. Otherwise, a typical phase diagram, as shown in Fig.2 for a usual multicomponent alloy series of soft magnetic materials, demonstrates formation of a glass only in a very narrow region. This is reproduced after the work of Inoue et al[17]. According to it, the largest value of ΔT_x = 49K is obtained at the $Fe_{74}Al_4Ga_2P_{12}B_4Si_4$ composition. A Fe-rich $Fe_{80}P_{12}B_4Si_4$ composition has a smaller ΔT_x = 36K. Simultaneous dissolution of Ga and Al with larger atomic sizes and large negative heat of mixing against the other constituent elements is, therefore, very effective for extension of the ΔT_x region before the crystallization at T_x.

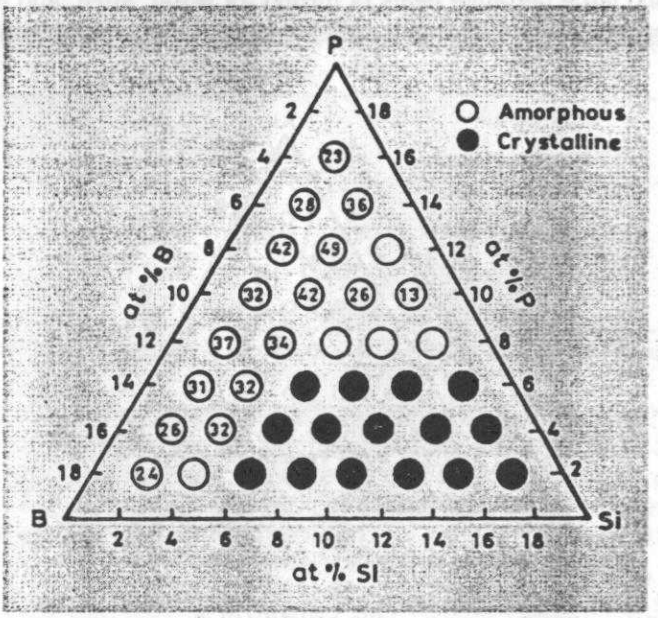

Fig. 2: Phase diagram in an amorphous phase formation (soft ferromagnetic) in $Fe_{74}Al_4Ga_2(P, B, Si)_{20}$ series. The numbers represent the temperature interval, $\Delta T = T_x - T_g$ of the supercooled region.

The alloy achieved with the extended ΔT_x = 49K is truly amorphous in nature and it involves a large value of enthalpy of relaxation ΔHrel in the T_g region in accord with the present results. The large value of ΔH_{rel} (e.g., 15 J/g observed in a typical $Nd_{60}Fe_{30}Al_{10}$ alloy) masks the relatively weak endothermic step of the T_g. It is, therefore, not visible in these examples. The excess DHrel releases with a prominent exothermic structural relaxation signal on heating the sample through it. In general, the DHrel signal is more prominent in the shear vitrified alloys. All these alloys exist in nonequilibrium metastable states far above their equilibrium energy states. The excess ΔH_{rel} energy, therefore, releases in an exothermic relaxation signal on heating the sample through it. In an isothermal heating, at T≤Tg, it results in a monotonically decreasing exothermic signal as a function of time. This has been studied and discussed with thermodynamic modeling in other reports in this series[35,36].

The hard ferromagnetic bulk amorphous alloys of the R-Fe-Al and R-Fe-Ga series present an exceptionally extended phase diagram of formation of a fully amorphous phase over a wide compositional range. For example, a typical phase diagram is given in Fig. 3 for the R-Fe-Al series. A thin amorphous ribbon easily forms at 0 to 90 at % Fe and 0 to 93 at % Al by rapid quenching as first reported by Inoue et al[16]. Also a bulk amorphous alloy forms over a pretty wide range of 20 to 40 at % Fe and 10 to 30 at % Al by copper mould casting and other methods[16]. The as cast ingots of the R-Fe-Al alloys, 4 to 5 mm diameter, by the arc melting in this work therefore have a smooth surface and a metallic luster at 20 to 40 at % Fe in formation of the amorphous phase. A systematic change in the atomic size of Nd>Fe>Al and large negative heats of mixing for Nd-Al, Al-Fe, and Nd-Fe atomic pairs seem to support a large GFA in this series as per the above four empirical rules.

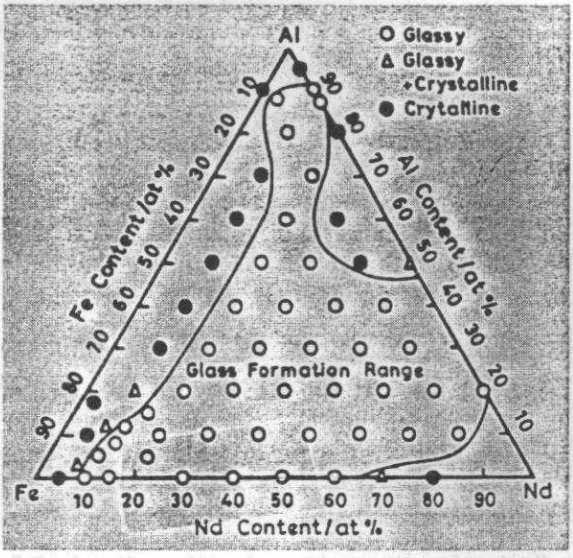

Fig. 3: Phase diagram in an amorphous hard ferromagnetic phase formation in Nd-Fe-Al series.

Magnetic properties

It is interesting to learn that the bulk amorphous $R_{90-x}Fe_xAl_{10}$ alloys exhibit optimal values of remanence Jr, saturation magnetization Js, energy-product (JH)max, and Curie temperature TC at a specific value of x ~ 30 irrespective to the R element. As given in Table 4, the alloy with R = Nd has the highest value of (JH)max = 19 kJ/m^3 with the highest value of TC = 610K. TC is a strong function of Fe-Fe, R-Fe and R-R exchange interactions in the magnetic R and Fe atoms in this series. As a result, it sensitively varies with a function of R as well as with a function of x in a given R-series. Pr($4f^2$), which has a smaller magnetic moment than Nd ($4f^3$), accounts for the smaller value of TC (515 K against 610 K at x~30) in the $Pr_{90-x}Fe_xAl_{10}$ alloy with respect to that in the $Nd_{90-x}Fe_xAl_{10}$ alloy (Table 4). Moreover, in thermomagnetograms, an increase in the value of x from (a) x = 20 to at (b) x = 30 in the $Nd_{90-x}Fe_xAl_{10}$ series leads to an increase in its TC-value by 60K with the final value of 610K. According to it, the Fe-Fe exchange interactions have a more pronounced effect on TC than the R-Fe or R-R exchange interactions. Very similar magnetic properties appear in $R_{90-x}Fe_xGa_{10}$ alloys

An especial advantage with the Pr-based alloys (in particular with a partial Al→Ga substitution) is that they are characteristically more oxidation-corrosion resistant than the Nd-based alloys in ambient atmosphere[9]. They, therefore, present their substantially stable magnetic properties. This is highly necessary for practical applications of these alloys in magnet technology and related devices and components. In this case, a partial substitution of Nd by Pr in the $(Nd_{1-y}Pr_y)_{90-x}Fe_xAl_{10}$ series thus could be a better alternative to have a practically useful bulk alloy with stable magnetic properties.

Table 4: Magnetic properties in hard ferromagnetic R-Fe-Al bulk amorphous $R_{90-x}Fe_xAl_{10}$ alloys

Composition	Magnetic Properties*			
	J_r(T)	H_c(kA/m)	$(JH)_{max}$(kJ/m^3)	T_c(K)
$Nd_{70}Fe_{20}Al_{10}$	0.08	239	13.0	550
$Nd_{60}Fe_{30}Al_{10}$	0.12	277	19.0	610
$Pr_{60}Fe_{30}Al_{10}$	0.09	300	13.0	515
$Er_{60}Fe_{30}Al_{10}$	0.10	280	12.0	590

** The optimal values appear in the amorphous bulk alloy at 30 at % Fe content.*

Conclusions

Bulk amorphous R-Fe-Al or R-Fe-Ga alloys form a new class of high-energy-density (HED) magnetic materials for permanent magnets and other applications. Because of large shape formability, they are easy to fabricate in thin plates, rods, cylinders, rings or any other shapes as desired in small devices and components. As compared to well-known $R_2Fe_{14}B$ intermetallics and other HED magnetic materials, the bulk amorphous alloys exhibit a relatively large electrical resistivity, which make them particularly suitable for applications in high frequency devices at a low power loss. The as-received bulk amorphous alloys of the two series present an energy-density as large as (JH)max ~ 19 kJ/m^3, i.e. comparable to that in the conventional high frequency ceramic magnets. Unusually, the recrystallized R-Fe-Al or R-Fe-Ga

alloys are extremely soft magnetic in nature and extremely hard in mechanical strength. Several unusual magnetic transitions appear at low temperatures in the virgin amorphous as well as in the recrystallized alloys with small crystallites of nanometer size. This is a subject of immense academic interest nowadays in understanding of magnetism and magnetic properties in correlated systems of small particles of quantum-confined dimension.

ACKNOWLEDGEMENTS

Financial support by a research grant from the DRDO, Government of India, is gratefully acknowledged.

REFERENCES :

1. K. Strnat, G. Hoffer, J. Olson, W. Ostertag and J.J. Becker, J. Appl. Phys. 38 (1967) 1001.
2. M. Sagawa, S. Fujimura, M. Togawa and Y. Matsuura, J. Appl. Phys. 55 (1984) 2083.
3. J.J. Croat, J.F. Herbst, R.W. Lee and F.E. Pinkerton, J. Appl. Phys. 55 (1984) 2078.
4. S. Ram, J. Magn. & Magn. Mater. 82 (1989) 129.
5. K. Schnitzke, L. Schultz, J. Wecker and M. Katter, Appl. Phys. Lett. 56 (1990) 587.
6. S. Ram and J.C. Joubert, J. Appl. Phys. 72 (1992) 1164.
7. S. Ram, Phys. Rev. B 49 (1994) 9632.
8. S. Ram, E. Claude and J.C. Joubert, IEEE. Trans. Magn. 31 (1995) 2200.
9. S. Ram, J. Mater. Sci. 32 (1997) 4133.
10. S. Ram, H.J. Fecht, S. Haldar, P. Ramachandrarao and H. D. Banerjee, Phys. Rev. B 56 (1997) 726.
11. S. Ram, Ind. J. Phys. 84A (2001) 379.
12. G. Kumar, J. Eckert, S. Roth, W. Loser, S. Ram and L. Schultz, J. Appl. Phys. 91 (2002) 3764.
13. K.H.J. Buschow, Meter. Report 1 (1986) 1.
14. W. Gong, H. Li, Z. Zhao and J. Chen, J. Appl. Phys. 69 (1991) 5119.
15. A. Inoue and J.S. Gook Zhang, Mater. Trans., JIM, 36 (1995) 1180 and ibid. 36 (1995) 1282.
16. A. Inoue, T. Zhang, A. Takeuchi and W. Zhang, Mater. Trans., JIM, 37 (1996) 636 and Mater. Trans., JIM, 37 (1997) 1731.
17. A. Inoue, A. Takeuchi and T. Zhang, Metall. Mater. Trans. 29A (1998) 177.
18. A. Inoue, A. Takeuchi and T. Zhang, Acta Mater. 48 (2000) 277.
19. S. Ram and H.J. Fecht, Mater. Trans., JIM, 41 (2000) 554.
20. P.S. Frankwicz, S. Ram and H.J. Fecht, Appl. Phys. Lett. 68 (1996) 2825.
21. W. Klement, R.H. Willens and P. Duwez, Nature 187 (160) 869.
22. H.S. Chen and D. Turnbull, J. Chem. Phys. 48 (1968) 2560.
23. H.S. Chen and D. Turnbull, Acta Met 17 (1969) 1021 and ibid. 22 (1974) 897.
24. S. Kavesh, in metallic glasses, Chapter 2, Ed. J.J. Gill-man and H.J. Leamy (ASM International Metal Park, OH 1978) P-36.
25. H.S. Chen, Acta Met. 22 (1974) 716.
26. A.L. Drehman, A.L. Greer and D. Turnbull, Appl. Phys. Lett. 41 (1982) 716.
27. H.W. Kui, A.L. Greer and D. Turnbull, Appl. Phys. Lett. 45 (1984) 615.
28. M.C.Lee, J.M. Kendall and W.L. Johnson, Appl. Phys. Lett. 40 (1982) 382.
29. A. Inoue, T. Zhang and T. Masumoto, Mater. Trans., JIM, 31 (1990) 177 and ibid. 31 (1990) 425.
30. A. Inoue, A. Kato, T. Zhang, S. G. Kim and T. Masumoto, Mater. Trans., JIM. 32 (1991) 609. 425.
31. A. Inoue, T. Nakamura, N. Nishiyama, and T. Masumoto, Mater. Trans.. JIM, 33 (1992) 937.
32. A. Peker and W. L. Johnson, Appl. Phys. Lett. 63 (1993) 2342.
33. W. L. Johnson, MRS Bull. 24 (1999) 42.
34. R.W. Cahn, in rapidly solidified alloys, Ed. H.H. Libermann (Marcel Decker, New York, 1993) P.1.
35. S. Ram and G.P. Johari, Phil. Mag. B 61 (1990) 299.
36. S. Ram, Phys. Rev. B 42 (1990) 9582.
37. P. Haasen, Physical Metallurgy (Cambridge Univ. Press, Cambridge, 1986) 125.